FIG. 3 Schematic representation of intercalation phenomena in cholic acid inclusion crystals as viewed down along the crystallographic b-axis. a, cholic acid only; b; cholic acid/acetophenone; and c, cholic acid/ethanol. x, y and z show unit distances (Å) of the axes in the rectangular coordinates.

We therefore interpret the phenomenon as intercalation of the guest molecules between the layers of host molecules. We based this on the comparison of the crystal structures before and after the absorption which reveal the following dynamical behaviour. First, the absorption of acetophenone molecules introduced a drastic change of the crystal structure; the absorbed guests forced the hosts to arrange so that channels appeared. Second, the change in cell dimensions is anisotropic, as shown in Fig. 3; the maximum variation is along the z-axis in which, the distance between layers increases from 8.5 Å to 11.7 Å. Third, the carboxylic groups exchanged partners from molecules on the adjacent layer to molecules which used to be their neighbours in the same layer. This results in the hydrogen-bonded network changing from a spiral arrangement to a cyclic one. After the absorption there are only weak van der Waals interactions between the layers. Fourth, the space group changed to $P2_1$ from $P2_12_12_1$, indicating that the steroidal molecules have to rotate in one layer but not in the neighbouring layers.

In case of ethanol, we confirmed the transformation by infrared spectroscopy. We believe that the ethanol molecules join the hydrogen-bonded networks and extend the crystallographic b-axis from 8.4-Å to 11.8 Å. There are no channels in this structure.

We have not found such a phenomenon in the case of deoxycholic acid. This is due to the fact that the host molecules form rigid and stable sheets of head-to-tail associations, and that the pure host crystal structure remains unknown,—the postulated structure containing no channel is based on theoretical calculation[9]. Therefore, cholic and deoxycholic acid provide an example of the great difference in the molecular assembly structure that can arise from a small difference in molecular structure.

We observed that the assembly of cholic acid can recognize organic guests in size, shape, polarity and chirality much more efficiently than that of deoxycholic acid. For example, the former can include[3] S-isomers of γ-methyl or γ-ethyl-γ-butyrolactone[3]. The X-ray crystal-structure analysis gave direct evidence for the chiral recognition (K. Miki et al., manuscript in preparation), indicating that the channels have chiral side pockets enough for accommodation of the chiral guests. In addition, we find that the accommodation space can change in size and shape through conformational changes of the flexible steroidal side chain and sliding of the layers to accommodate guest molecules. We have already ascertained that cholic acid has more than six different kinds of molecular assembly modes. Guest-responsive molecular assemblies such as these may provide a very simple analogue for studying the guest-responsive behaviour of macromolecules such as antibodies.

We believe that this is the first demonstration of intercalation in organic crystals, as compared with those of inorganic compounds such as graphite and clay. Although it is well known that macromolecules in biological systems acquire large amounts of information in the process of molecular evolution, and express their information as dynamical, reversible, environment-dependent, three-dimensional structures suitable for molecular rec-

ognition, the expression of molecular information by small molecules has not hitherto been discussed. The behaviour of the molecular assemblies of cholic acid mentioned above are conceptually similar to those of the macromolecules. It seems that small molecules such as cholic acid can express their molecular information through the behaviour of the assemblies, but not as single molecules. Perhaps such assemblies of small molecules had a role in the process of molecular evolution.

Further systematic research for the intercalation crystals of organic hosts would be useful for the design of new molecular assemblies with guest-responsive and dynamical structures having accurate molecular recognition for organic compounds. □

1. Miyata, M., Shibakami, M., Goonewardena, W. & Takemoto, K. Chemy Lett. 605–608 (1987).
2. Miki, K. et al. J. Am. chem. Soc. 110, 6594–6596 (1988).
3. Miyata, M., Shibakami, M. & Takemoto, K. JCS chem. Commun. 655–657 (1988).
4. Johnson, P. L. & Schaefer, J. P. Acta crystallogr. B28, 3083–3089 (1972).
5. Lessinger, L. Crystal Struct. Commun. 11, 1787–1792 (1982).
6. Whittingham, M. S. & Jacobson, A. J. (eds) Intercalation Chemistry (Academic, New York, 1982).
7. Atwood, J. L., Davies, J. E. D. & MacNicol, D. D. (eds) Inclusion Compounds (Academic, London, 1984).
8. Herndon, W. C. J. chem. Educ. 44, 724–727 (1967).
9. Giglio, E. in Inclusion Compounds (eds Atwood, J. L., Davies, J. E. D. & MacNicol, D. D.) Vol. 2, 207 (Academic, London, 1984).
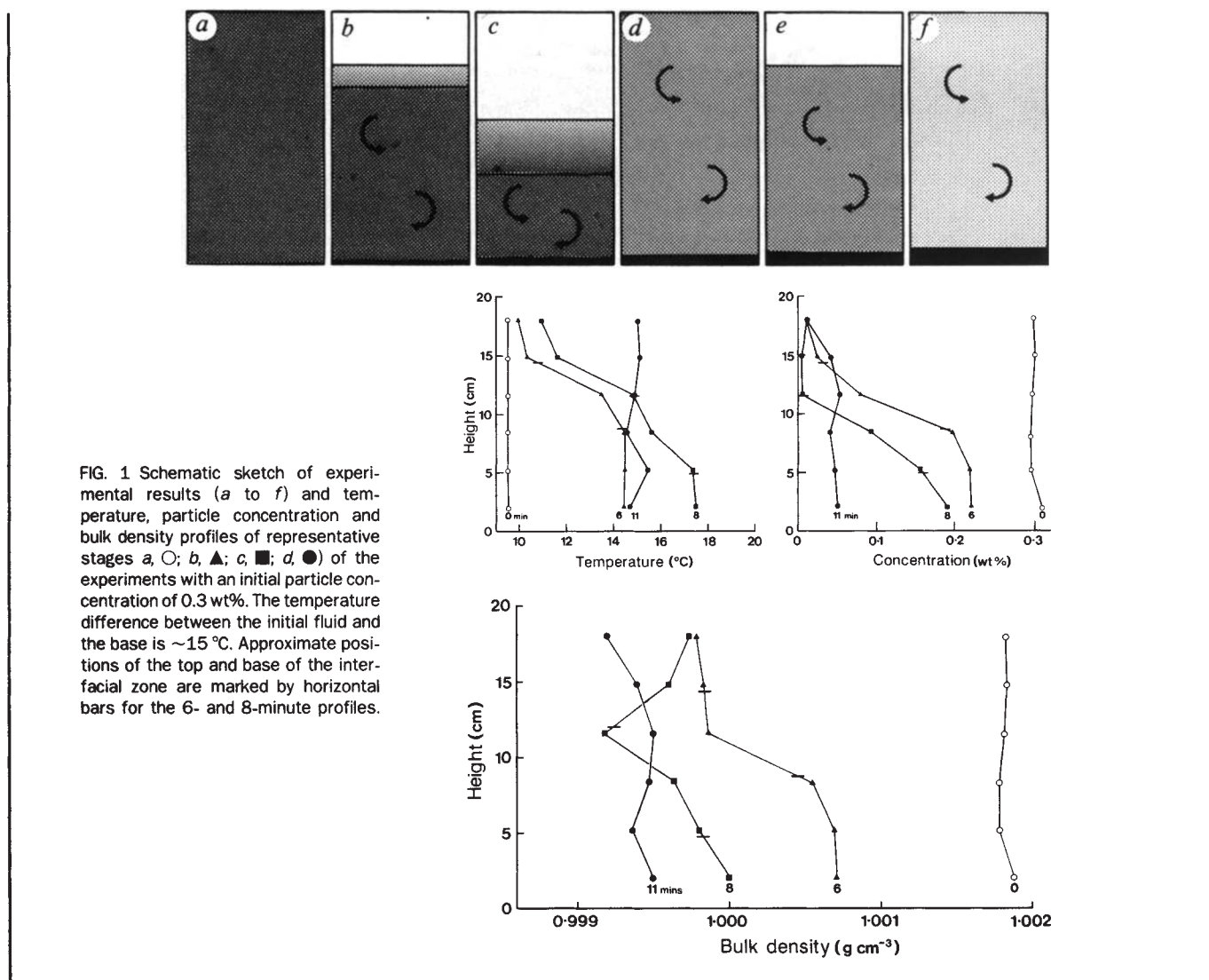
Sedimentation of particles from a convecting fluid

Takehiro Koyaguchi*‡, Mark A. Hallworth*, Herbert E. Huppert* & R. Stephen J. Sparks†

* Institute of Theoretical Geophysics, University of Cambridge, 20 Silver Street, Cambridge CB3 9EW, UK
† Department of Geology, Wills Building, University of Bristol, Bristol BS8 1RJ, UK

THE sedimentation of particles from a convecting fluid is a process of much interest to engineers, fluid dynamicists, geologists and metallurgists. For example, the process plays a fundamental role in controlling the settling behaviour of phenocrysts in magma chambers, crystals and impurities in metallic castings and carbon microparticles in combustion chambers. Previous studies of particle settling in convecting systems[1–5] have assumed that the concentration of particles is so small that their presence does not modify the convective motion. Here we present experimental results which show that convective motion due to heating from below can be affected by the presence of particles and is controlled by the bulk density of a particulate suspension, which is a function of

‡ Permanent address: Department of Geology, Faculty of Science, Kumamoto University, Kumamoto 860, Japan.

FIG. 1 Schematic sketch of experimental results (a to f) and temperature, particle concentration and bulk density profiles of representative stages a, ○; b, ▲; c, ■; d, ●) of the experiments with an initial particle concentration of 0.3 wt%. The temperature difference between the initial fluid and the base is ~15 °C. Approximate positions of the top and base of the interfacial zone are marked by horizontal bars for the 6- and 8-minute profiles.

both temperature and particle concentration. Above a certain concentration, the particle distribution initially stabilizes the bulk density gradient during sedimentation, and convection is confined to a sedimenting layer beneath a clear layer. Eventually, however, the destabilizing thermal gradient exceeds the stabilizing effect of the particles, and a sudden overturn of the whole system results. Our experimental results agree with a simple physical model.

We carried out experiments in a tank ($20 \times 20 \times 20$ cm deep) heated from below. The tank was filled with a mixture of water and well sorted silicon carbide powder ($16 \mu m$ in median diameter with a standard deviation of $\sim 3 \mu m$, particle density $\rho_p = 3.217$ g cm^{-3}). The Stokes settling velocity for this range of particle size is $0.02-0.05$ cm s^{-1}, giving a Reynolds number of $\sim 10^{-3}$. The initial temperature difference between the fluid and the base was typically $5-15$ °C, which leads to Rayleigh numbers of up to 10^9. The particles were initially distributed uniformly throughout the tank and were then left to settle. Temperatures and particle concentrations were monitored at several heights by thermistors and an optical transmission device[6] respectively. At least two distinct regimes of settling behaviour were observed for different initial particle concentrations.

At very low initial concentrations (<0.01 wt%), particles were distributed nearly uniformly throughout the tank; deposition occurred at the base and the particle concentration decreased exponentially with time[5]. In our experiments with higher (but still fairly small) initial particle concentrations (~0.3 wt%), turbulent convection throughout the whole tank was suppressed

and confined to a suspension layer beneath a sharply defined descending interface.

Schematic sketches and profiles of temperature, particle concentration and bulk density for representative stages of the experiment are shown in Fig. 1. Settling of particles created a clear layer separated from the underlying suspension layer by an interfacial zone (Fig. 1b). The interfacial zone descended at a rate approximately equal to the Stokes settling velocity, and increased in thickness with time mainly as a result of the small variation in particle size and hence in settling velocity (Fig. 1b, c). In the lower suspension layer, temperature and particle concentrations were nearly uniform because of convective mixing; the temperature increased and the particle concentration decreased with time. In the interfacial zone, the temperature and particle concentration decreased with increasing height. This zone was stagnant, because the stabilizing particle concentration gradient was sufficient to overcome the opposing thermal gradient and thus to produce a stable bulk density stratification. The temperature of the upper clear layer, which was insulated from the lower layer by the stagnant interfacial zone, increased only slightly during this stage.

The bulk density of the lower suspension layer decreased with time, as its temperature increased and its particle concentration decreased (Fig. 1). Furthermore, as the interfacial zone descended and became wider, the density gradient in this zone decreased. Eventually it became unstable, and the whole system overturned (about 10 minutes after the start of the experiment),

re-establishing uniform temperature and concentration profiles throughout the tank (Fig. 1d). The homogenized particle concentration after overturn was much lower ($\sim$0.05 wt%) than the the initial concentration because of sedimentation at the base. This cycle was repeated several times (Fig. 1e,f), with the homogenized concentration decreasing after each overturn and with the time interval between each overturn decreasing. Eventually, the concentration became so low that particles settled with uniform concentrations and temperatures throughout the tank, in the same way as in the low-particle-concentration regime.

We have developed a simple physical model of this phenomenon based on the experimental observations. We consider the particles to be of uniform size and to be suspended in a fluid undergoing vigorous convection by being heated from the base at a constant temperature, T_b. The suspension layer decreases in depth with time, leaving a clear layer above. When the volume fraction of particles is small, the descent rate can be approximated by the Stokes settling velocity for a single particle, v_s. We assume that there is a sharp interface between the two layers, which thermally insulates the upper clear layer from the lower suspension layer. The temperature of the upper layer is at the initial value, T_0, and its density is thus at the initial fluid density, ρ_i.

The bulk density of the lower layer, ρ_1, can be expressed as

$$\frac{1}{\rho_1} = \frac{C}{\rho_p} + \frac{1-C}{\rho_i\{1-\alpha(T_1-T_0)\}} \qquad (1)$$

where C is the particle concentration expressed as a mass fraction, ρ_p is the density of the particles, α is the coefficient of thermal expansion and T_1 is the temperature of the lower layer. The density of the lower layer decreases with time as T_1 increases. When it becomes less than the density of the upper layer, ρ_i, overturn occurs. When $C \ll 1$, the critical temperature at the overturn, T_1^*, is approximated from equation (1) as

$$T_1^* = \frac{C(\rho_p - \rho_i)}{\alpha\rho_p} + T_0 \qquad (2)$$

Under the above conditions, the heat flux from the base to the lower layer can be expressed as[7]

$$q = \rho_f c_p \gamma \left(\frac{\alpha g \kappa^2}{\nu}\right)^{1/3} (T_b - T_1)^{4/3} \qquad (3)$$
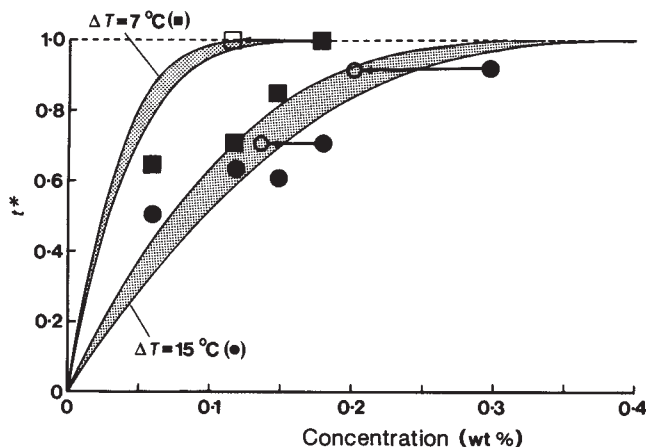

FIG. 2 Theoretical and experimental values of normalized timescale for overturn ($t^* = v_s t/h_0$) plotted against particle concentration for two temperature differences between the initial fluid and the base ($\bullet$, experiments with $\Delta T = 15$ °C; $\blacksquare$, experiments with $\Delta T = 7$ °C). The shaded regions envelope the theoretically calculated values for a reasonable range of settling velocities, that is, 0.025–0.035 cm s^{-1} when $\Delta T = 15$ °C and 0.030–0.040 cm s^{-1} when $\Delta T = 7$ °C. Arrows from solid to open symbols indicate (where measured) the decrease in concentration of the lower layer from the initial value (solid) to that just before overturn (open).

where ρ_f is the fluid density, c_p is the specific heat, κ is the thermal diffusivity, g is the acceleration due to gravity, ν is the kinematic viscosity and γ is a dimensionless constant, the value of which is determined empirically to be $\sim$0.1 at relatively high Rayleigh numbers[8]. The heat conservation equation for the lower layer is

$$q = c_p \rho_f (h_0 - v_s t)\frac{dT_1}{dt} \qquad (4)$$

where h_0 is the height of the fluid layer. From equations (3) and (4), the temperature of the lower layer as a function of time can be expressed as

$$T_1(t) = T_b - \left\{ -\frac{\gamma}{3v_s}\left(\frac{\alpha g \kappa^2}{\nu}\right)^{1/3} \ln\left(1 - \frac{v_s t}{h_0}\right) \right. $$
$$\left. + (T_b - T_0)^{-1/3} \right\}^{-3} \qquad (5)$$

The temperature, T_1, increases with time to a critical value, T_1^*, and then overturn occurs.

We define t^* ($= v_s t/h_0$) as the timescale for overturn divided by the timescale for the interface to reach the base, which is a suitably normalized timescale for overturn. From equations (2) and (5), t^* is given by

$$t^* = 1 - \exp\left[-\frac{3v_s}{\gamma}\left(\frac{\nu}{\alpha g \kappa^2}\right)^{1/3} \right.$$
$$\left. \times \{(T_b - T_1^*)^{-1/3} - (T_b - T_0)^{-1/3}\}\right] \qquad (6)$$

This quantity provides a criterion for the overturn behaviour of the fluid: if $t^* \ll 1$, overturns occur continuously, whereas if $t^* > 1$, overturn does not occur before all the particles have reached the floor.

In Fig. 2 we plot calculated and experimentally determined values of t^* against particle concentration for two specific initial temperature differences between the fluid and the base. The model calculations agree fairly well with the experiments. In our idealized model, particle concentration in the lower layer is constant, because particles will settle out with the same velocity as the interface descends. In reality, however, this concentration decreases with time, mainly because of variation in particle size. The interface velocity lies somewhere between the settling velocities of the smallest and largest particles, so that the larger particles are progressively removed from the sedimenting layer[9]. The agreement between theory and experiment is improved if the concentration just before overturn is used rather than the initial concentration. The timescale increases with increasing particle concentration and with decreasing temperature difference between the base and fluid. When the particle concentration is very small, $T_1^* \approx T_0$ (see equation (2)), and hence t^* is small (see equation (6)). As C increases, $T_1^* \approx T_b$, and hence t^* approaches 1. Because T_1^* cannot be greater than T_b, overturn does not occur if

$$C > \frac{\alpha(T_b - T_0)\rho_p}{\rho_p - \rho_i} \equiv \frac{\alpha\Delta T}{r_\rho} \qquad (7)$$

where r_ρ is $(\rho_p - \rho_i)/\rho_p$. This implies that $t^* < 1$ only when the particle concentration is so low that the increase in bulk density due to particle suspension ($C(\rho_p - \rho_i)/\rho_p \equiv Cr_\rho$) is compensated by the decrease in fluid density due to increasing temperature at the bottom ($\alpha(T_b - T_0) \equiv \alpha\Delta T$).

These experimental results indicate an important feature of sedimentation that has not been hitherto recognized. The settling behaviour of particles has previously been accounted for only in terms of the ratio of the particle settling velocity to the vertical component of convective velocity. If the convective velocity exceeds the settling velocity, particles behave like passive tracers of the fluid motion[3-5]. Our results suggest, however, that an

additional factor needs to be taken into account, namely the ratio of the decrease in fluid density due to increasing temperature ($\alpha \Delta T$) to the increase in bulk density due to particle suspension (Cr_p).

Although the experiments were carried out in a simplified system, the basic principle expressed by equation (7) is believed to be applicable to natural situations. The main difference is that in our experiments convection is driven by heating from below whereas in natural systems (such as magma chambers) it can be driven both thermally and compositionally at the roof, floor and side walls. Preliminary experiments involving cooling from above suggest that compositional and thermal gradients are established and can lead to overturn and rehomogenization of the particle-laden fluid in a manner similar to that of heating from below. There are some important quantitative differences, however, between the two cases, such as the strength of convection in the upper layer and the thermal evolution of both layers. In the geological context our results suggest that the presence of relatively small amounts of phenocrysts can have a significant influence on the convective motion in a magma chamber, and can provide a mechanism for periodic overturn and rehomogenization of thermal and compositional gradients in an evolving magma body. Such phenomena may also have important consequences for the settling of crystals or impurities in metallurgical casting processes. □

1. Bartlett, R. W. *Am. J. Sci.* **267**, 1967–1982 (1969).
2. Huppert, H. E. & Sparks, R. S. J. *Contr. Miner. Petrol.* **75**, 279–289 (1980).
3. Marsh, B. D. & Maxey, M. R. *J. Volcanol. geotherm. Res.* **24**, 95–150 (1985).
4. Weinstein, S. A., Yuen, D. A. & Olson, P. L. *Earth planet. Sci. Lett.* **87**, 237–248 (1988).
5. Martin, D. & Nokes, R. *Nature* **332**, 534–536 (1988).
6. Davis, R. H. & Hassen, M. A. *J. Fluid Mech.* **196**, 107–134 (1988).
7. Turner, J. S. *Buoyancy Effects in Fluids* (Cambridge University Press, 1973).
8. Denton, R. A. & Woods, I. R. *Int. J. Heat Mass Transfer* **22**, 1330–1346 (1979).
9. Davis, R. H. & Birdsell, K. H. *A.I.Ch.E. Jl* **34**, 123–129 (1988).

Evidence from rare gases for magma-chamber degassing of highly evolved mid-ocean-ridge basalt

David E. Fisher* & Michael R. Perfit†

* Marine Geology and Geophysics, Rosenstiel School of Marine and Atmospheric Science, University of Miami, Florida 33149, USA
† Department of Geology, University of Florida, Gainesville, Florida 32611, USA

HIGHLY evolved lavas have been recovered from moderate- to fast-spreading centres along the mid-ocean ridge system, most commonly near propagating rifts and overlapping spreading centres[1-7]. Their origin and occurrence are generally explained by extensive modification of a primary basalt magma by fractional crystallization at shallow levels in the oceanic crust (model 1)[1-4,6-9]. Other crustal processes have also been invoked, including periodic magma mixing of a highly fractionated liquid with multiple primary liquids (model 2)[10,11], and seawater interaction with the mantle-derived magma (model 3)[12-14]. Here we report the first ^{4}He and argon isotope data for several highly evolved mid-ocean-ridge basalts (MORBs) and andesites. The samples were recovered with the submersible *Alvin* from a very limited section ($<$8 km^2) of the axial valley of the eastern Galapagos Rift, between 85°52' and 85°50' W. Although they range in composition from moderately evolved normal (N) MORB to ferrobasalts, Fe–Ti basalts and high-silica andesites, geochemical studies indicate that the suite

is cogenetic, facilitating interpretation of the data[15]. We find distinct differences in the rare-gas data between the evolved and N-MORBs, indicating that the evolved magmas have undergone pre-eruption degassing in a process not common to the source magmas for normal MORBs. Our data fit well with model 1, but provide no evidence for models 2 and 3.

It is well known that the rare gases in N-MORB glasses are dominated by a component derived from the mantle source, because their isotopic composition is distinctly different from crustal materials. Most notably, they are characterized by high ^{3}He/^{4}He and ^{40}Ar/^{36}Ar relative to the atmosphere. Also, N-MORBs typically have large amounts of ^{4}He and ^{40}Ar which cannot be accounted for by decay of U, Th and K after eruption, and ^{4}He/^{40}Ar ratios greater than the production ratio of 1–3. (Subaerial rocks have ^{4}He/^{40}Ar ratios lower than the production ratio because of diffusive loss.) Typical MORBs have ^{4}He contents of 10^{-5}–10^{-6} cm^3 STP g^{-1} and ^{40}Ar$_r$ contents of $\sim$$10^{-6}$ cm^3 STP g^{-1} (where the subscript r refers to the radiogenic component), with ^{4}He/^{40}Ar$_r$ ratios of 5–25 (ref. 16 and references therein). The N-MORB samples reported here fit this pattern (Table 1), which shows that the Galapagos MORB source is typical of those previously sampled (ref. 16 and references therein). The evolved samples, however, have ^{4}He contents of only 10^{-8} cm^3 STP g^{-1}, ^{40}Ar$_r$ contents of $\sim$$10^{-7}$ cm^3 STP g^{-1} and ^{4}He/^{40}Ar$_r$ ratios of $<$0.1. The low absolute values measured in the evolved samples indicate loss of mantle gases (relative to N-MORB). The low ^{4}He/^{40}Ar$_r$ ratios indicate that diffusive loss is the most likely process.

Loss of the mantle gases in the evolved samples is also demonstrated in Fig. 1, in which ^{40}Ar/^{36}Ar is plotted against $1/^{36}$Ar. If the measured gases consist of a constant amount of trapped mantle ^{40}Ar mixed with varying amounts of an atmospheric component, the data should be described by a straight line with an intercept of 295 (ref. 16). Previously measured MORB glasses from a variety of locations are well fit by straight lines[16], as are the three N-MORB measured here ($r^2 = 0.998$, where r is the correlation coefficient), indicating that the total argon components do consist of a single mantle component mixed with varying amounts an atmospheric-like component. The data from the evolved samples are not as well fit by a straight line ($r^2 = 0.83$) and the slope is significantly lower. This indicates a loss of the mantle component variably from sample to sample combined with a variable atmospheric component, and lower trapped ^{40}Ar, respectively. Total amounts of the atmospheric component, as measured by the total ^{36}Ar contents, are well within the range of all MORB data[16] and do not vary
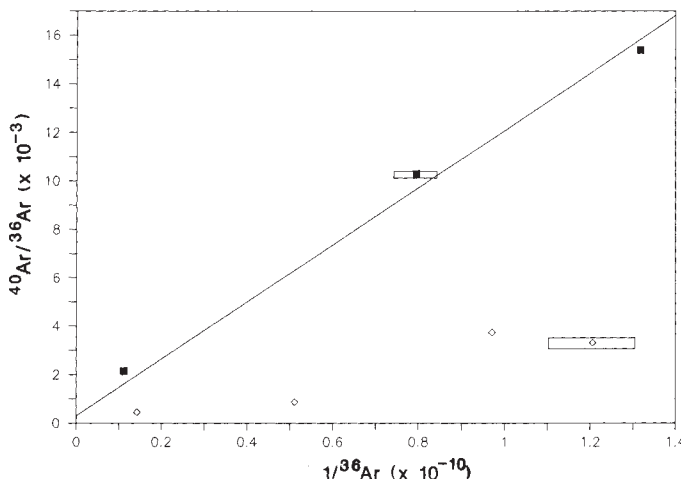

FIG. 1 ^{40}Ar/^{36}Ar plotted against $1/^{36}$Ar. The straight line is the least-squares fit to the MORB points (■), constrained to pass through the atmospheric ratio of 295. The evolved basalts (◇) lie below the line. Circumscribed rectangles indicate limits of error on typical data points.